RSC Advances

ROYAL SOCIETY OF CHEMISTRY

www.rsc.org/advances

Journal Name

RSCPublishing

ARTICLE

Au/graphene oxide/carbon nanotube flexible catalyst film: synthesis, characterization and its application for catalytic reduction of 4-nitrophenol

Fan Yang,[a‡] Chunxia Wang,[b‡] Lina Wang,[a] Chao Liu,[a] Andong Feng,[a] Xue Liu,[a] Cheng Chi,[a] Xilai Jia,[a] Liqiang Zhang,[a] Yongfeng Li[a*]

Cite this: DOI: 10.1039/x0xx00000x

Received 00th January 2012,
Accepted 00th January 2012

DOI: 10.1039/x0xx00000x

www.rsc.org/

We report a simple approach for fabricating flexible, free-standing, and catalytic film composed of graphene oxide/carbon nanotube-Au (GO/CNT-Au) composites by using a one-pot chemical reduction route. The catalyst film was characterized by scanning electron microscopy, transmission electron microscopy, X-ray diffraction, X-ray photoelectron spectroscopy, thermogravimetric analysis and Raman spectroscopy to investigate the morphology, crystalline structure of the composites. The layered structure of the catalyst film is porous, flexible and exhibits excellent catalytic property in the reduction of 4-nitrophenol (4-NP) to 4-aminophenol (4-AP) reaction. This study demonstrate here for simple yet effective synthesis of catalyst film with a number of advantages such as good strength, high stability, easy operation, and good reusability with minimal loss of activity.

Introduction

As representatives of novel carbon nanomaterials, graphene sheets and their tubular variants carbon nanotubes (CNTs) have been normally used as an ideal support for the dispersion and stabilization of metal nanoparticles, due to their large chemically active surface, high surface to volume ratio, unique physical properties, inherent size and stability at high temperatures.[1-6] Meanwhile, gold nanoparticles using in catalysis has attracted attention due to their physical and chemical properties and their potentially green and sustainable catalytic properties.[7-9] Therefore, a large number of synthetic methods such as photolysis, electroless deposition, electrodeposition, chemical decoration π-π stacking, electrostatic interactions, sonochemistry, microwave assisted, plasma, adsorption, deposition-precipitation, wet impregnation, or by other means for synthesis of Au nanoparticles on carbon nanotubes and graphene have been developed.[10-13] Moreover, carbon nanomaterials supported Au nanoparticles possesses a high stability and catalytic efficiency has been commonly utilized as heterogeneous catalyst in organic molecule transformation reactions.[10,14-18] In particular, the reduction of 4-nitrophenol (4-NP) over Au nanocatalyst in the presence of $NaBH_4$ has been intensively investigated for the efficient production of 4-aminophenol (4-AP).[19-21] The 4-NP is highly toxic and shows detrimental effects on human health and environment as toxic and mutagenic substance, on the other hand, aside from being an important intermediate in the preparation of several analgesic and antipyretic drugs, such as paracetamol, acetanilide and phenacetin, 4-AP has also been applied as photograph developer, corrosion inhibitor, anti-corrosion lubricant and hair-dyeing agent.[22-24] Therefore, the efficient production of 4-AP from reduction of 4-NP has been intensively investigated.

Recently, large-scale production of both graphene and CNT are being actively pursued in industry and both are now commercially available at low cost through a chemical oxidation and reduction process using graphite as a raw material, and through a chemical vapour deposition method.[25] However, the as-produced two-dimensional graphene and one-dimensional CNT are usually presented in powder form, which tend to the obvious reduction of available surface area due to their aggregate and restack.[26,27] In order to minimize the restacking-induced surface area loss, great efforts have been made to design and construct innovative composites. Recently, graphene and CNT are usually used together to build the three-dimensional (3D) interconnected network by chemical vapour deposition,[28-30] layer-by-layer electrostatic self-assembly,[31-33] electrophoretic assembly,[34,35] vacuum filtration,[36,37] spray method and spin-coating method,[38,39] in situ chemical reduction

[a]*State Key Laboratory of Heavy oil Processing, China University of Petroleum, Changping 102249, Beijing, China. Fax: +86-10-89739028; Tel: +86-10-89739028; E-mail: yfli@cup.edu.cn*

[b]*Beijing National Laboratory for Molecular Sciences, Key Laboratory of Analytical Chemistry for Living Biosystems, Institute of Chemistry, the Chinese Academy of Science, Beijing 100190, China*

‡ These authors contributed equally.

† Electronic supplementary information (ESI) available: Au nanoparticle size, Au loading, apparent reaction rates, reaction time, TOF values for Au catalysts.

method,[40,41] or by other means.[42,43] The 3D carbon nanomaterials comprise of CNT which can hinder the self-aggregation of graphene sheet and the composite of graphene sheet can separate the CNT bundles, thus endowing the 3D carbon composite with an ultrahigh surface-to-volume ratio. Due to these significant advantages, the 3D carbon nanomaterials have been widely applied in transparent conductive thin film, anodes for lithium ion batteries, super capacitors, solar cells, biomedicine, microwave absorption, and catalysis support.[44-50]

Herein, we report the synthesis of flexible, robust and catalytic film using a one-pot chemical reduction route to decorate GO/CNT with Au nanoparticles by a mechanical mixing method. The GO/CNT composite demonstrated here shows several advantages: first, it is more efficient to support the Au nanoparticles than GO and CNTs. Second, the mechanical strength of GO/CNT is better than GO and CNT, which can produce the flexible catalytic film. Third, the amphiprotic support arises from hydrophilic GO and hydrophobic CNT which can gather the organic compounds in the water. Fourth, the catalyst film can be recovered easily form the reaction mixture. The catalytic performance of the composites is investigated detailed by the reduction of 4-NP reaction. The as-prepared GO/CNT-Au shows higher catalytic activity than that of GO supported Au nanoparticles and CNT supported Au nanoparticles. Moreover, the catalyst can be reused ten times without significant loss of catalytic activity.

Experimental section

Materials

All chemicals were used as received without further purification: graphite powder (200 mesh) (Alfa Aesar, Johnson Matthey Company); $HAuCl_4 \cdot 4H_2O$ (Sinopharm Chemical Reagent Beijing Co., Ltd); 1-methyl-2-pyrrolidone (C_5H_9NO) (Aladdin Industrial Corporation); $KMnO_4$, H_2O_2, ethanol, methylene chloride (CH_2Cl_2), acetone, acetic ether, tetrahydrofuran, toluene, N, N-Dimethylformamide (DMF) (Beijing chemical works).

Preparation of graphene oxide

GO was synthesized from graphite powder according to a modified Hummer's method. Typically, a mixture of concentrated H_2SO_4/H_3PO_4 (60 mL: 6.6 mL) was added to a flask containing graphite powder (500 mg) and $KMnO_4$ (3 g), and heated to 50 °C and stirred for 12 h. After that, the reaction was cooled down to room temperature and poured into an ice bath (~40 mL). Then, 30% H_2O_2 (~2.5 mL) was added drop wise with stirring. The mixture was centrifuged and sequentially washed with 100 mL HCl (0.04 g mL^{-1}), deionized water to remove residual unexfoliated graphite and oxidant agents. The remaining solution was dialyzed for one week to eliminate excess ions. Then, the obtained graphite oxide was dispersed in water and subsequently ulltrasonicated (120 W, 40 kHz) for 3 h to form GO. Eventually, the final product was dried.

Preparation of GO/CNT-Au composites

In a typical synthesis of the nanohybrids, 15 mg of the as-synthesized GO was dispersed in 50 mL deionized water to yield yellow brown solution by ultrasonication (120 W, 40 kHz). Then 15 mg of CNTs and 100 mL 1-methyl-2-pyrrolidinone (NMP) were added into a homogenizer to stir vigorously for 1 h. Subsequently, the above GO aqueous was added and stirred for 30 min to get the homogenous GO/CNT suspension. Then, the suspension was transferred into 250 mL round-bottom flask, to the mixture of the suspension were added 7 mg $HAuCl_4 \cdot 4H_2O$ dissolved in 5 mL deionized water with mechanical stirrer for 30 min, the 10.5 mg $NaBH_4$ aqueous solution was added and the mixture was stirred for 3h. The mixture was filtrated to remove the excess impurities and washed with ethanol by a centrifuge process. The different samples of GO/CNT can be obtained by adjusting different weights of GO and CNT. The GO supported Au nanoparticles and CNT supported Au nanoparticles were synthesized by the same method. The samples with different weight fractions (1/2, 1/1, 2/1) of GO/CNT support Au nanoparticles were labelled as G/C-Au-1, G/C-Au-2, G/C-Au-3, and the GO supported Au nanoparticles and CNT supported Au nanoparticles were labelled as G-Au, C-Au. The flexible catalyst film made from free-standing GO/CNT-Au was prepared by filtrating the above solution through nylon organic membrane filters, followed by washing, air drying and peeling off from the filters.

Catalytic reduction of 4-NP in micro-reaction vial

In a typical catalysis reaction in micro-reaction vial, G/C-Au-2 catalyst, corresponding to a percentage of Au of 0.5 mmol% with respect to 4-NP was used, and 14.0 mg 4-NP (0.1 mmol) and 1.0 mg G/C-Au-2 catalyst were mixed together in 1 mL miliQ-water then stirred for 1 min in order to mix thoroughly in a micro-reaction vial. Subsequently, 378 mg $NaBH_4$ (10 mmol) in 3 mL miliQ-water was added into the above solution by vigorous magnetic stirring. After that, 10 µl of the reaction mixture was collected and diluted to 3 ml with miliQ-water for UV-vis measurement every 30 s. UV-vis absorption spectra were recorded to monitor the change in the reaction mixture over the range from 200 to 500 nm at room temperature. The catalytic reactions performed for the conversion of 4-NP to 4-AP using the other Au catalysts were carried out under the same conditions. Each run of the recycling G/C-Au-2 was carried out under identical conditions, and the reusing G/C-Au-2 was recovered by filtering off the solution of the previous run after finishing the reaction.

Characterization of the catalyst

The morphology and the size of the synthesized samples were characterized by scanning electron microscopy (SEM; FEI Quanta200F) and transmission electron microscopy (TEM, FEI, F20) combined with an energy dispersive X-ray spectroscopy (EDS) at an acceleration voltage of 200 kV. X-ray diffraction

(XRD, Bruker D8 Advance Germany) was applied to characterize the crystal structure of the hybrid materials, and the data was collected on a Shimadzu XD-3A diffractometer using Cu Kα radiation. The X-ray photoelectron spectroscopy (XPS, Thermo Fisher K-Alpha American with an Al K α X-ray source) was used to measure the elemental composition of samples. Raman spectra were recorded with a Renishaw in via confocal Raman microscope system using green (532 nm) laser excitation. Thermogravimetric analysis (TGA) profiles were obtained between 30 ^{o}C and 800 ^{o}C in O_2 using a Mettler Toledo TGA/DSC 1 instrument. The heating rate was 10 ^{o}C/min. UV-vis absorption spectra of the samples were recorded at room temperature on a TU-1900 apparatus.

Results and discussion

Fig. 1 shows the process flow to fabricate the GO/CNT-Au. First, a simple mechanical mixing method is employed for constructing the supports, consisting of integration and dispersion in nanoscale dimensions of GO and CNTs, which can make the composites of the support hierarchical and porous. The GO in the designed support could reduce the interconnection between the CNTs bundles, and the restacking of GO sheets could be weaken due to the interspersed CNTs existing in the intercalated of GO sheets. Moreover, the synthesized support shows amphipathic property induced by synergistic contributions of the hydrophilic GO and hydrophobic CNTs. Second, a one-pot chemical reduction route is used to prepare GO/CNT-Au. Finally, the flexible, free-standing GO/CNT-Au film can be obtained by vacuum filtration.

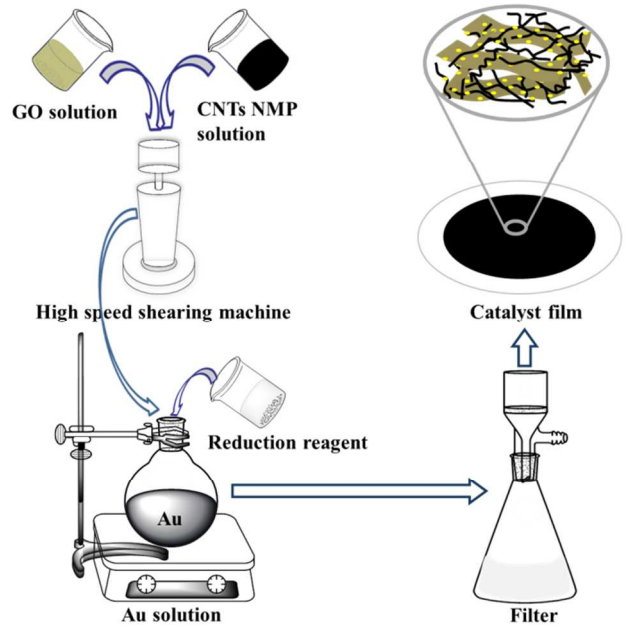

Fig. 1 The synthesis process of GO/CNT-Au composites

The structures and morphologies of the synthesized hybrid composites are characterized by SEM and TEM (Fig. 2 and Fig. 1S). Fig. 2a shows the G/C-Au-2 film is porous and a sandwich like structure, some CNT is exposed on the surface of the GO sheets, and some are embedded in the inter-layers of the GO sheets. TEM analysis for the sample obtained from the synthesized materials reveals that the successive decrease in the amount of GO leads to the Au aggregation phenomenon. The result is in agreement with the decrease in the Au particle size after addition of the GO in the support, and the mean particle sizes of G/C-Au-1, G/C-Au-2, G/C-Au-3, G-Au and C-Au are 2.5 nm, 2.9 nm, 1.4 nm, 4.1 nm and 4.9 nm respectively, as shown in Fig. S2 and summarized in Table S1. The high-resolution TEM (HRTEM) image is shown in Fig. 2d, which demonstrates the crystalline nature of Au nanoparticles, the lattice fringe distances of 0.205 nm and 0.235 nm can be assigned to the (200) and (111) planes of the crystalline cubic Au, and the angle of (200) and (111) planes is 55.6^{o} which match well with 54.7^{o} of the calculation value.

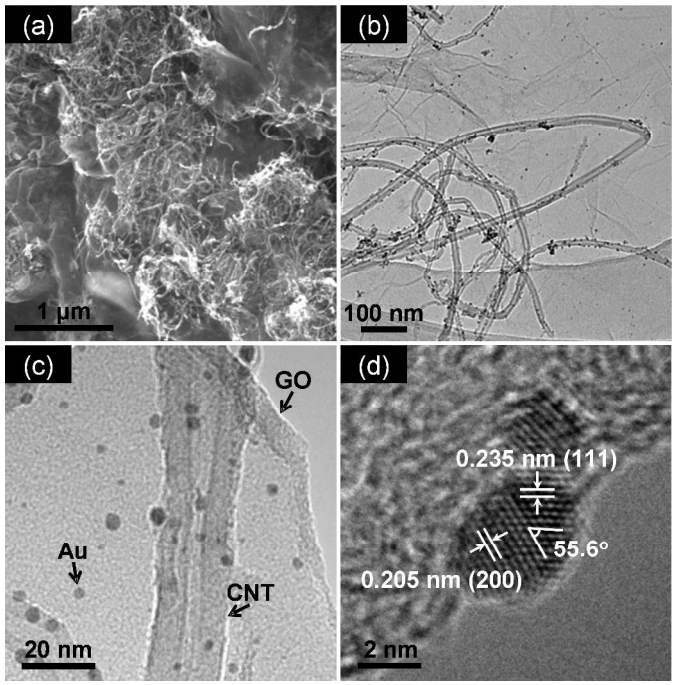

Fig. 2 A SEM image (a); TEM images (b), (c) of G/C-Au-2; a HRTEM image (d) of G/C-Au-2

The XRD pattern of G/C-Au-2 is shown in Fig. 3a, indicating the crystalline structure of the synthesized sample. The broad diffraction peaks from 5^{o} to 9^{o} and from 22^{o} to 28^{o} of the nanocomposites correspond to the (002) plane of GO and the (002) plane of CNTs, respectively. The characteristic diffraction peaks at 38.3^{o}, 44.6^{o}, 64.7^{o}, 77.7^{o} and 81.6^{o} correspond to Au (111), (200), (220), (311) and (222) reflections of crystalline Au (0) (JCPDS no. 04-0784), respectively. Furthermore, Fig. 3b shows the selected area electron diffraction (SAED) image for the G/C-Au-2, and the diffraction rings of lattice planes are in agreement with XRD results. Another powerful technique for studying and identifying the nanohybrids is XPS, the bands in the wide scan confirm the presence of C1s, O1s and Au4f as shown in Fig. 3c,

which is in agreement with the EDX results as shown in Fig. S2(f), the peaks at 284.08 and 531.08 eV which are attributed to C1s and O1s of C/G-Au-2. Two peaks in XPS for $Au4f_{7/2}$ and $Au4f_{5/2}$ at 83.3 and 86.9 eV are attributed to Au4f, the Au contents are estimated by XPS to be 8.36 wt.% which is in agreement with the amount of Au input. We have taken XPS-peak-imitating analysis of Au4f of G/C-Au-1, G/C-Au-2, G/C-Au-3, G-Au and C-Au in order to analyze the oxidation state of the Au species. All above catalysts show two peaks for $Au4f_{5/2}$ and $Au4f_{7/2}$ which are split into two types of Au electronic states (Au^0 and Au^{+1}), as shown in Fig. 3d and Fig. S3.

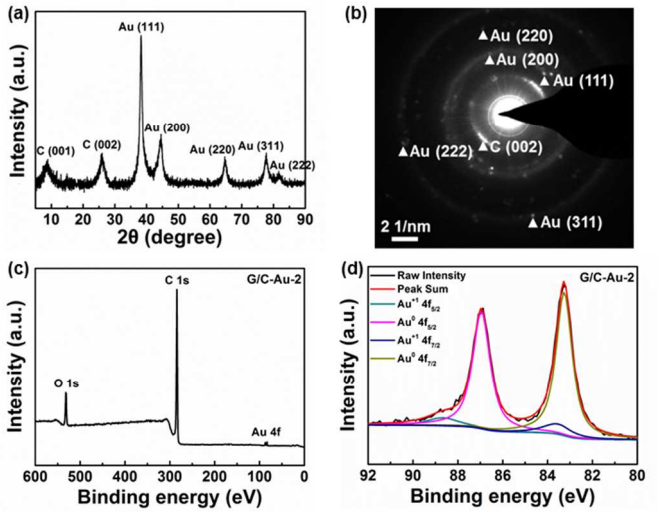

Fig. 3 XRD pattern (a), SEAD pattern (b), and XPS spectra of G/C-Au-2 (c), high-resolution XPS spectra of Au 4f of G/C-Au-2 (d).

The Raman spectra of GO-Au, CNTs-Au and G/C-Au showing several feature peaks can be seen in Fig. 4a. The G peak at 1590 cm^{-1} is due to the normal vibration mode, which relates to the relative motion of C sp^2 atoms. The D band which can be seen at 1330 cm^{-1} is related to a disorder-induced mode. The G/C-Au composites show a similar value of the ratio of D-band to G-band intensity compared with the GO/CNTs composites, which indicates that the reduction of the Au salt during the synthetic procedure has little effect on the surface properties of the supports, thus we could change the hydrophobic and hydrophilic properties of the supports through regulating the ration of GO and CNTs. The TGA curves are used to quantify the amount of Au in the composites as shown in Fig. 4b, the Au contents of G/C-Au-1, G/C-Au-2, G/C-Au-3 are 11.1 wt.%, 9.8 wt.%, 9.4 wt.%, respectively. The Au contents of G-Au and C-Au are 19.6 wt.% and 24.0 wt.% which may be due to the loss of support during the purification procedure.[51] Three primary mass loss processes are observed, first step below 180 ^oC could be attributed to the evaporation of adsorbed water, and second step from 180 ^oC to 410 ^oC can be assigned to the oxidation of graphene, and the third step between 410 ^oC to 605 ^oC indicates the decomposition of CNT. It is noticed that the third weight loss of G/C-Au-1, G/C-Au-2, G/C-Au-3 curve also can reflect the component change which in agreement with the ratio of GO to CNT in the support.

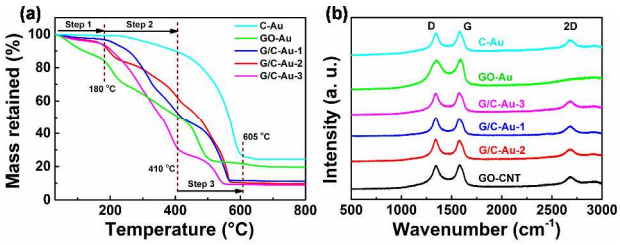

Fig. 4 Raman spectra (a), TGA curves (b) of C-Au, GO-Au and G/C-Au-1, G/C-Au-2, G/C-Au-3

In order to evaluate the efficiency of the as-prepared Au catalysts, we first employ the reduction of 4-NP to 4-AP in the presence of a hydrogen source, $NaBH_4$. Initially, the 4-NP solution has a light yellow color, which turns dark yellow after the addition of $NaBH_4$ due to the formation of 4-nitrophenolate (Fig. S4a). However, the dark yellow color gradually fades away with the progression of the reduction to 4-AP (Fig. S4b). Although $NaBH_4$ is well known as a strong reductant, the reduction of 4-NP is quite slow. Although GO/CNT is introduced into the reaction process, the reaction rate does not show any considerable progress. Thus, catalysts are usually needed to accelerate the conversion rate of 4-NP to 4-AP. The catalytic performance of Au catalysts is assessed in micro-reaction vial as described in the experimental part, as shown in Fig. 5. The intensity of the absorption band at 400 nm decreases gradually with time increasing. At the same time, a new absorption peak at 300 nm appears as shoulders, being ascribed to the formation of 4-AP. Moreover, the two isosbestic points are observed at 280 and 312 nm, suggesting that the two principal species are responsible for the conversion reaction. On the basis of the UV/vis spectra, therefore, the pseudo-first-order reaction kinetics is applied to determine the apparent reaction rate, K_{app}, for the reaction. The K_{app} for the G/C-Au-1, G/C-Au-2, G/C-Au-3 are as high as 0.75, 0.34, 0.22 min^{-1}, respectively. As a comparison, the G-Au and C-Au are utilized as catalysts for the catalytic hydrogenation of 4-NP, the K_{app} values are 0.16 and 0.12 min^{-1}. These results clearly indicate that the combined GO and CNT support has great effects on the catalytic activity. Additionally, the K_{app} is dependent on the amount of catalyst, but it is not directly related to the catalytic activity of the catalysts, whereas, the turnover frequency (TOF) is a significant parameter for evaluating the catalytic activity in heterogeneous catalytic reaction. The TOF value for the G/C-Au-2 is as high as 3015 h^{-1}, which is higher than 819 h^{-1} and 1571 h^{-1} for G/C-Au-1 and G/C-Au-3, indicating that the GO/CNT ratio in the support could influence the catalytic activity, we propose the distinction of the catalytic activity of these catalysts is due to the hydrophilic-hydrophobic properties of the supports. The GO makes the support hydrophilic and the CNT makes the support lipophilic, and maybe the GO/CNT ratio with 1/1 enable $NaBH_4$ and 4-NP to gather onto the surface of the low-coordinated Au atoms in H_2O more easily. Compared with other related Au heterogeneous catalysts reported recently, such as GO/TWEEN 20-Au (126 h^{-1} of TOF),[52] GO/SiO_2-Au (1028 h^{-1} of TOF),[53] graphene hydrogel-

Au (12 h^{-1} of TOF),[54] the G/C-Au-2 catalyst demonstrates obviously superior catalytic activity.

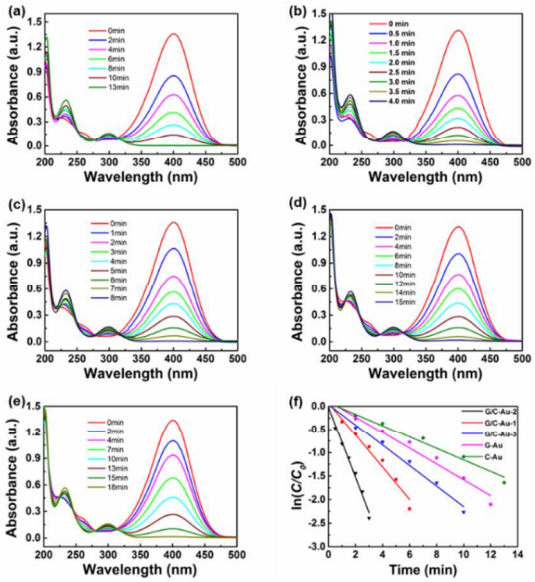

Fig. 5 Successive absorption spectra of the conversion from 4-NP to 4-AP with powder Au catalysts: G/C-Au-1 (a), G/C-Au-2 (b), G/C-Au-3 (c), G-Au(d), C-Au (e); (f) plots of $\ln(C/C_0)$ versus time for the conversion from 4-NP to 4-AP with Au catalysts.

Reusability is an important feature for a heterogeneous catalyst, which is better than a homogenous one. First, in order to confirm that the reaction is indeed catalyzed by the solid G/C-Au-2 rather than homogenous Au species, leaching test has been carried out after the catalytic reduction of 4-NP is proceeded for 1 min under standard conditions. After that the reaction mixture without catalyst is separated, and no further reaction takes place after removing the catalyst. In addition, the leaching of the Au has been also examined using ICP-OES, and no leaching of Au is detected. To assess recyclability of G/C-Au-2, multiple 4-NP reduction cycles have been carried out, the G/C-Au-2 has been repeatedly used for 10 times as shown in Fig. 6, the conversion of 4-NP can be completed with increasing of the reaction time from 4 min to 8 min. The first-order rate constant (K_{app}) decreases slightly from 0.75 to 0.46 min^{-1}. Moreover, the TEM image of the catalyst after reaction indicates that the particle size and the morphology the Au nanoparticles shows no detectable change, suggesting that the

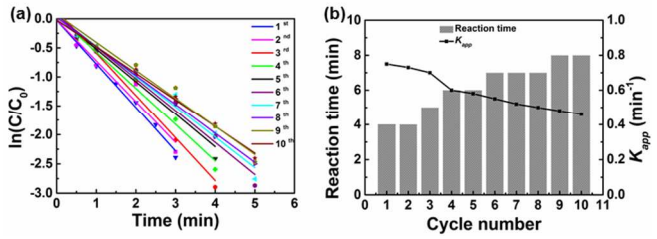

Fig. 6 Plots of $\ln(C/C_0)$ versus time for 10 cycles of the conversion from 4-NP to 4-AP with G/C-Au-2 catalyst; (b) the reaction time and K_{app} of the G/C-Au-2 during 10 cycles of the 4-NP reduction reaction.

hybrid composite maintain high stability (Fig. S6).

Due to the high catalytic activity of G/C-Au-2, we also fabricate the catalytic film of G/C-Au-2 as shown in Fig. 7a and 7b show the synthesized catalyst film is flexible, and the catalytic activity of as-prepared catalyst film has been evaluated by reducing 4-NP to 4-AP, there are large amounts of bubbles generated in the reaction solution after addition of the Au catalyst film as shown in Figs. S5a and S5b, the catalyst film could be easily separated by taking the catalyst out of the reaction solutions, the macroscopic morphology before and after the reaction are shown in Fig. S5d and S5e. Fig. S5d shows the catalyst could place horizontal without bending, indicating that the catalytic film is very light due to its porous structure, after reaction, the wet recycle catalytic film can carry itself without brokenness, indicating that the catalytic film shows good strength. The K_{aap} value of the synthesized catalytic film is 0.042 min^{-1} as shown in Figs. 7c and 7d.

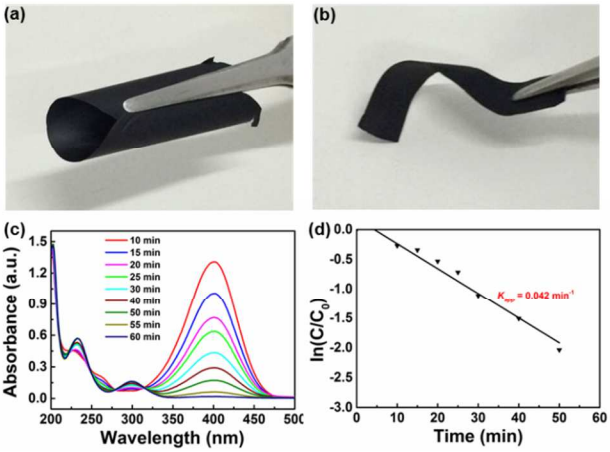

Fig. 7 Images showing that the catalytic film is flexible (a and b), successive absorption spectra of the conversion from 4-NP to 4-AP with G/C-Au-2 catalytic film (c), (f) plots of $\ln(C/C_0)$ versus time for the conversion from 4-NP to 4-AP with G/C-Au-2 catalytic film.

Conclusions

In conclusion, we have developed an efficient and general synthetic approach for the synthesis of GO/CNT-Au hybrid materials. The synthesized GO/CNT-Au is confirmed by SEM, TEM, XRD and XPS characterizations, which offers numerous advantages, such as more efficient to support the Au nanoparticles, excellent strength, and good hydrophilic-hydrophobic properties. The hybrid materials as new catalyst is applied for reduction of 4-NP to 4-AP reaction. Moreover, the results indicate that the GO/CNT-Au catalyst exhibits higher catalytic activity than GO-Au and G-Au catalysts, and the G/C-Au-2 catalyst can be reused several times without leaching and significant loss of activity. It is worth noting that the current catalyst could be easily for fabricating flexible, free-standing, and catalytic film of GO/C-Au composite, which makes the catalyst recovered from the reaction solution easily. Further work is in progress to extend this concept to synthesize

GO/CNT supported other metal nanoparticles as catalysts for organic molecular transformations.

Acknowledgements

This work was financially supported by the National Natural Science Foundation of China (Nos. 21202203, 21322609, 21106184), Science Foundation of China University of Petroleum, Beijing (Nos. YJRC-2013-31, 2462014QZDX01) and Thousand Talents Program.

Notes and references

1. F.M. Koehler, W.J. Stark, *Accounts Chem. Res.*, 2012, **46**, 2297-306.
2. L.M. Ombaka, P. Ndungu, V.O. Nyamori, *Catal. Today,* 2013, **217**, 65-75.
3. J. Zhu, A. Holmen, D. Chen. *ChemCatChem*, 2013, **5**, 378-401.
4. E. Lam, J.H. Luong, *ACS Catal.,* 2014, **4**, 3393-3410.
5. P. Trogadas, T.F. Fuller, P. Strasser, *Carbon*, 2014, **75**, 5-42.
6. X. Zhou, J. Qiao, L. Yang, J. Zhang, *Adv. Energy Mater.*, 2014, **4**, 1301523-48.
7. M. Stratakis, H. Garcia, *Chem. Rev.*, 2012, **112**, 4469-506.
8. A. Majdalawieh, M.C. Kanan, O. ElKadri, S.M. Kanan. *J Nanosci. Nanotechno.*, 2014, **14**, 4757-80.
9. X. Liu, L. He, Y. Liu, Y. Cao, *Accounts Chem. Res.*, 2013, 47, 793-804.
10. A. Corma, H. S. Garcia, *Chem. Soc. Rev.*, 2008, 37, 2096-126.
11. T. Liu, F. Yang, Y. Li, L. Ren, L.Q. Zhang, K. Xu, X. Wang, C. Xu, J. Gao, *J Mater. Chem. A*, 2014, 2, 245-250.
12. M. Cittadini, M. Bersani, F. Perrozzi, L. Ottaviano, W. Wlodarski, A. Martucci, *Carbon*, 2014, **69**, 452-459.
13. H. Duan, D. Wang, Y. Li. *Chem. Soc. Rev.*, 2015, DOI: 10.1039/C4CS00363B.
14. J. Goebl, J.B. Joo, M. Dahl, Y. Yin, *Catal. Today*, **2014**, 225, 90-95.
15. B.S. Takale, M. Bao, Y. Yamamoto, *Org. Biomol. Chem.*, 2014, **12**, 2005-2027.
16. P. Pachfule, S. Kandambeth, D. Diaz, R. Banerjee, *Chem. Commun.*, 2014, **50**, 3169-3172.
17. N. Linares, C.P. Canlas, J. Garcia-Martinez, T.J. Pinnavaia, *Catal. Commun.*, 2014, **44**, 50-53.
18. M. Tang, X. Wang, F. Wu, Y. Liu, S. Zhang, X. Pang, X. Li, H Qiu, *Carbon*, 2014, **71**, 238-248.
19. P. Zhang, C. Shao, X. Li, M. Zhang, X. Zhang, C. Su, N. Lu, K. Wang, Y. Liu, *PCCP*, 2013, 15, 10453-10458.
20. Z. Dong, X. Le, Y. Liu, C. Dong, J. Ma, *J Mater. Chem. A*, 2014, 2, 18775-18785.
21. Z. Dong, X. Le, C. Dong, W. Zhang, X. Li and J. Ma, *Appl. Catal. B-Environ.,* 2015, 162, 372-380.
22. S. Saha, A. Pal, S. Kundu, S. Basu, T. Pal, *Langmuir*, 2009, **26**, 2885-2893.
23. Z. Jiang, J. Xie, D. Jiang, X. Wei, M. Chen, *CrystEngComm*, 2013, **15**, 560-569.
24. Y. Du, H. Chen, R. Chen, N. Xu, *Appl. Catal. A-Gen.*, 2004, **277**, 259-264.
25. F. Wei, Q. Zhang, W.Z. Qian, H. Yu, Y. Wang, G. Luo, G. Xu, D. Wang, *Powder Technol.*, 2008, **183**, 10-20.
26. W. Yang, Z. Gao, J. Wang, J. Ma, M. Zhang, L. Liu, *ACS Appl. Mater. Inter.*, 2013, **5**, 5443-5454.
27. H. Gao, F. Xiao, C.B. Ching, H. Duan, *ACS Appl. Mater. Inter.*, 2012, **4**, 7020-7026.
28. S.W. Hong, F. Du, W. Lan, S. Kim, H.S. Kim, J.A. Rogers, *Adv. Mater.*, 2011, **23**, 3821-3826.
29. X. Zhu, G. Ning, Z. Fan, J. Gao, C. Xu, W. Qian, F. Wei, *Carbon*, 2012, **50**, 2764-2771.
30. M. Nagatsu, T. Yoshida, M. Mesko, A. Ogino, T. Matsuda, T. Tanaka, H. Tatsuoka, K. Murakami, *Carbon*, 2006, **44**, 3336-3341.
31. T.K. Hong, D.W. Lee, H.J. Choi, H.S. Shin, B.S. Kim. *ACS Nano*, 2010, **4**, 3861-3868.
32. H.R. Byon, S.W. Lee, S. Chen, P.T. Hammond, Y. Shao-Horn, *Carbon*, 2011, **49**, 457-67.
33. J. Lee, Y.K. Kim, D.H. Min, *J. Am. Chem. Soc.*, 2010, **132**, 14714-14717.
34. H. Beitollahi, I. Sheikhshoaie, *J. Electroanal. Chem.*, 2011, *661*, 336-342.
35. S.D. Seo, I.S. Hwang, S.H. Lee, H.W. Shim, D.W. Kim, *Ceram. Int.*, 2012, **38**, 3017-3021.
36. L. Qiu, X. Yang, X. Gou, W. Yang, Z. Ma, G.G. Wallace, D. Li, *Chem-Eur. J.*, 2010, **16**, 10653-10658.
37. X. Lu, H. Dou, B. Gao, C. Yuan, S. Yang, L. Hao, L. Shen, X. Zhang, *Electrochim. Acta.*, 2011, **56**, 5115-5121.
38. W.S. Jang, S.S. Chae, S.J. Lee, K.M. Song, H.K. Baik, *Carbon*, 2012, **50**, 943-51.
39. J. Kim, V.C. Tung, J. Huang, *Adv. Energy Mater.*, 2011, **1**, 1052-1057.
40. Z. Zheng, Y. Du, Z. Wang, F. Zhang, C. Wang, *J. Mol. Catal. A-Chem.*, 2012, **363-364**, 481-488.
41. S. Woo, Y.R. Kim, T.D. Chung, Y. Piao, H. Kim, *Electrochim. Acta.*, 2012, **59**, 509-514.
42. X. Dong, Y. Ma, G. Zhu, Y. Huang, J. Wang, M.B. Chan-Park, L. Wang, W. Huang, P. Chen, *J. Mater. Chem.*, 2012, **22**, 17044-17048.
43. Y. Wu, T. Zhang, F. Zhang, Y. Wang, Y. Ma, Y. Huang, Y. Liu, Y. Chen, *Nano Energy*, 2012, **1**, 820-827.
44. D.H. Lee, J.A. Lee, W.J. Lee, S.O. Kim, *Small*, 2011, **7**, 95-100.
45. G. Zhou, L. Yin, D. Wang, L. Li, S. Pei, I.R. Gentle, F. Li, H. Cheng, *ACS Nano*, 2013, **7**, 5367-5375.
46. S. Yang, K. Chang, H.W. Tien, Y.F. Lee, S. Li, Y. Wang, J. Wang, C.C. M. Ma, C.C. Hu, *J. Mater. Chem.*, 2011, *21*, 2374-2380.
47. S. Li, Y. Luo, W. Lv, W. Yu, S. Wu, P. Hou, Q. Yang, Q. Meng, C. Liu, H. Chen, *Adv. Energy Mater.*, 2011, **1**, 486-490.
48. L. Wang, X. Jia, Y. Li, F. Yang, L. Zhang, L. Liu, R. Xiao, H. Yang, *J. Mater. Chem. A*, 2014, **2**, 14940-14946.
49. X. Fan, G. Jiao, L. Gao, P. Jin, X. Li, *J. Mater. Chem. B*, 2013, **1**, 2658-2664.
50. T. Sun, Z. Zhang, J. Xiao, C. Chen, F. Xiao, S. Wang, Y. Liu, *Sci. rep.*, 2013, **3**, 2527-1-5.
51. J. Song, L. Xu, R. Xing, Q. Li, C. Zhou, D. Liu, H. Song, *Sci. rep.*, 2014, 7515-1-4.
52. W. Lu, R. Ning, X. Qin, Y. Zhang, G. Chang, S. Liu, Y. Luo, X. Sun, *J. Hazard. Mater.*, 2011, 197, 320-326.
53. C. Zhu, L. Han, P. Hu, S. Dong, *Nanoscale*, 2012, 4, 1641-1646.
54. J. Li, C. Y. Liu, Y. Liu, *J. Mater. Chem.*, 2012, 22, 8426-8430.

Graphic abstract

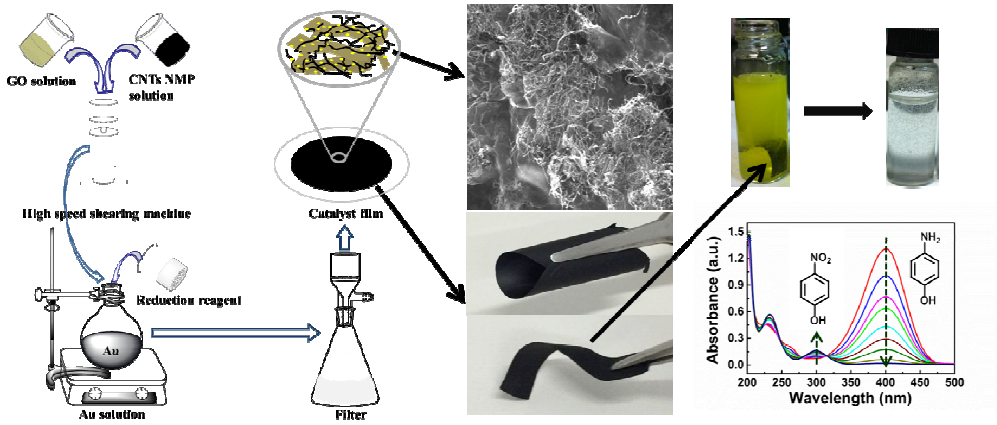

We report a simple approach for fabricating flexible, free-standing, and catalytic film composed of graphene oxide/carbon nanotube-Au (GO/CNT-Au) composites by using a one-pot chemical reduction route. The layered structure of the catalyst film is porous, flexible and exhibits excellent catalytic property in the reduction of 4-nitrophenol (4-NP) to 4-aminophenol (4-AP) reaction. The catalyst film could be easily separated by taking the catalyst out of the reaction solutions, and the catalyst can be reused several times without leaching and significant loss of activity.